Calculation of the Average Properties of Atoms in Molecules. II

Friedrich W. Biegler-König, Richard F. W. Bader, and Ting-Hua Tang*

Department of Chemistry, McMaster University, Hamilton, Ontario, Canada L8S 4M1
Received 28 September 1981; accepted 10 November 1981

This article describes an algorithm for the calculation of the average properties of an atom in a molecule. The atom is defined within the topological theory of molecular structure, a theory which defines atoms, bonds, structure, and structural stability in terms of the topological properties of a system's charge distribution. The average properties of the atom so defined are uniquely determined by quantum mechanics. Results for a number of hydrocarbon molecules, obtained by the program PROAIM (properties of atoms in molecules) which implements this algorithm, are given. In general, this program enables one to calculate the average energy of an atom in a molecule to an accuracy of ±1 kcal/mol.

I. INTRODUCTION

This article describes an algorithm for the calculation of the average properties of an atom in a molecule. The atom is defined by a topological property of the molecular electronic charge density $\rho(\mathbf{x})$. As a consequence of this identification of an atom with a particular region of real space, one obtains a complete theory of molecular structure. This theory has been previously described[1,2] and recently reviewed.[3,4] We give here only the elements of the theory essential to the development of the algorithm. This necessitates a brief account of the properties of the gradient vector field of the charge density.

II. GRADIENT VECTOR FIELD OF THE CHARGE DENSITY

Figure 1 displays the gradient vector fields of the charge distributions for the molecules cyclopropane and tetrahedrane through the trajectories of $\nabla\rho$. Each of these trajectories, called a gradient path, is the integral curve of the differential equation,

$$d\mathbf{x}(s)/ds = \nabla\rho[\mathbf{x}(s)] \qquad (1)$$

for some initial value $\mathbf{x}(0) = \mathbf{x}_0$. Thus the points $\mathbf{x}(s)$ of the gradient path through $\mathbf{x}_0$ are given by

$$\mathbf{x}(s) = \mathbf{x}_0 + \int_0^s \nabla\rho[\mathbf{x}(t)]dt \qquad (2)$$

Alternatively, eq. (1) can be reexpressed in terms of the path length l—the arc length along a gradient path—to yield

$$d\mathbf{x}/dl = \nabla\rho(\mathbf{x})/|\nabla\rho(\mathbf{x})| \qquad (3)$$

The essential topological properties of ρ can be summarized by the complete specification of its critical points, points where $\nabla\rho = 0$. These can be of two types: at a nondegenerate or rank-three critical point, $\mathbf{x}_c$, the Hessian matrix of $\rho, H(\rho) = [H_{ij}(\rho)]$, is of maximal rank, i.e.,

$$\det [H(\rho)]_{\mathbf{x}=\mathbf{x}_c} \neq 0$$

with

$$H_{ij}(\rho) = \partial^2\rho/\partial x_i \partial x_j$$

At a degenerate critical point, $\det [H(\rho)]$ vanishes, since $H(\rho)$ is of a rank less than three at such a point. A nondegenerate critical point, $\mathbf{x}_c$, is further characterized by its signature σ, defined as the excess number of positive over negative eigenvalues of $H(\rho)_{\mathbf{x}=\mathbf{x}_c}$. Thus a nondegenerate critical point is one of the types $(3,\sigma)$ where $\sigma = -3,-1,+1,+3$ and the first number within the parentheses denotes its rank.

A $(3, -3)$ critical point exhibits the properties which define an attractor of the gradient vector field of the charge distribution: a closed subset $A \subset R^3$ is an attractor of $\nabla\rho$, if and only if (i) it is invariant to the flow of $\nabla\rho$, (ii) any trajectory whose origin lies in A is contained in A, (iii) there exists an open invariant neighborhood B of A such that any trajectory originating in B terminates at A. The largest neighborhood B_{max} satisfying this condition is called the basin of A.

* Permanent address: Department of Chemistry, Tianjin Teachers' College, Tianjin, People's Republic of China.

A

B

C
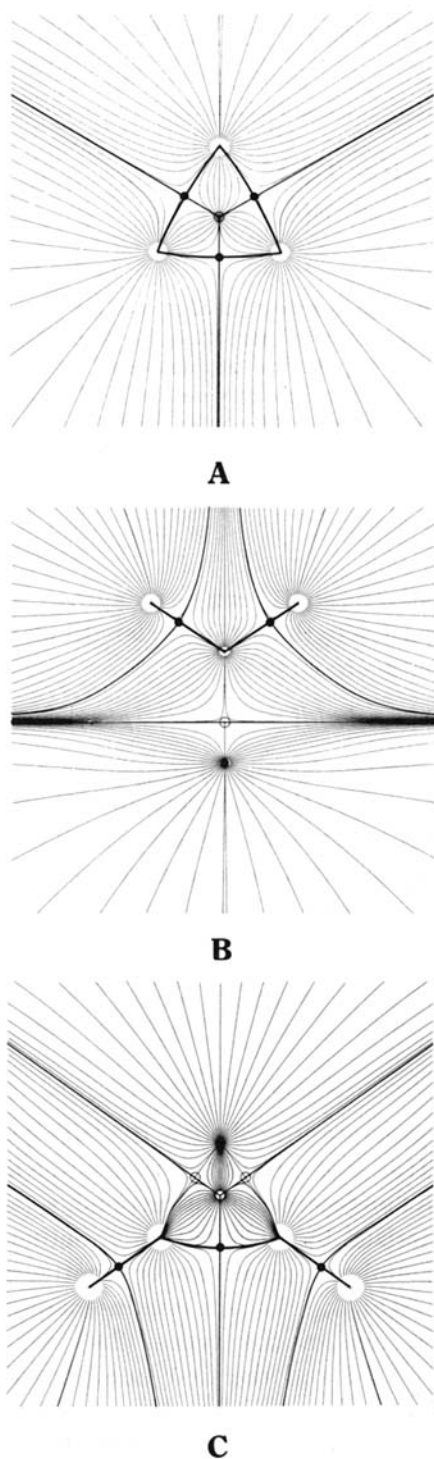
Figure 1. Display of the trajectories of $\nabla\rho(\mathbf{r})$ for cyclopropane, C_3H_6 (A and B), and tetrahedrane, C_4H_4 (C). The trajectories are terminated at the surface of a small sphere of arbitrary radius centered on each nucleus. (A) is for the plane containing the three carbon nuclei. There are three $(3,-1)$ or bond critical points denoted by solid circles and a $(3,+1)$ or ring critical point, denoted by an open circle. The bond paths linking nuclei are shown as bold lines, the interatomic surfaces as less bold lines. The plane shown in (B) is perpendicular to the one illustrated in (A). It contains the nuclei and bond paths of one CH_2 group. The lower solid circle is the position of the bond critical point between the out of plane carbon atoms. The trajectories terminating at this point define the associated carbon-carbon interatomic surface. The unique axis of the ring critical point

Since the only closed subsets of R^3 exhibiting these properties are the singletons determined by the local maxima in the charge distribution which occur at the positions of the nuclei, the nuclei act as the attractors of the gradient vector field of $\rho(\mathbf{x})$. The result of this identification is that the space of the molecular charge distribution, real space, is partitioned into disjoint regions, the basins, each of which contains one and only one point attractor or nucleus. This fundamental topological property of a charge distribution is illustrated in Figure 1. *An atom, free or bound, is defined as the union of an attractor and its associated basin.*

Alternatively, the atom can be defined in terms of its boundary. The basin of a single nuclear attractor in an isolated atom covers the entire three-dimensional space R^3. For an atom in a molecule the atomic basin is an open subset of R^3. It is separated from neighboring atoms by interatomic surfaces. The existence of an interatomic surface S_{AB} denotes the presence of a $(3,-1)$ critical point: the surface S_{AB} consists of all gradient paths which terminate at the $(3,-1)$ critical point. It is generated by the two eigenvectors $\mathbf{v}_1$ and $\mathbf{v}_2$ associated with the negative eigenvalues of the Hessian matrix of such a critical point. Indeed, in a sufficiently small neighborhood of the critical point at $\mathbf{x}_c$, the interatomic surface coincides with its tangent plane at $\mathbf{x}_c$, which is linearly spanned by $\mathbf{v}_1$ and $\mathbf{v}_2$. The entire interatomic surface can be obtained by solving the differential equation, eq. (1), for initial conditions $\mathbf{x}_0 = \mathbf{x}(0)$, such that each $\mathbf{x}_0$ belongs to the intersection of the surface with the above neighborhood of $\mathbf{x}_c$, and is thus expressible as a linear combination of $\mathbf{v}_1$ and $\mathbf{v}_2$. We define the *atomic surface* S_A of an atom A as the boundary of its basin. Hence $S_A \supset U_B S_{AB}$. Generally this boundary comprises the union of a number of interatomic surfaces, separating two neighboring basins, and some portions which may be infinitely distant from the attractor. The interatomic surfaces as well as the surfaces found at infinity are the only closed surfaces S of R^3 which satisfy the equation

$$\nabla\rho(\mathbf{x}) \cdot \mathbf{n}(\mathbf{x}) = 0 \ \forall \mathbf{x} \in S \qquad (4)$$

where $\mathbf{n}$ is the unit vector normal to the surface at $\mathbf{x}$.

is shown in (B). The plane shown in (C) contains an H—C—C—H nuclear framework of C_4H_4. The central critical point is a $(3,+3)$ or cage critical point. The upper bond critical point lies between the two out-of-plane carbon atoms. Also shown are two ring critical points. Note that in C_4H_4 the ring surfaces, as well as the carbon–carbon bond paths are outwardly curved.

A surface which satisfies eq. (4) is called a *zero-flux surface*. Thus, an atom is a region of real space which contains a single nuclear attractor and which is bounded by a zero-flux surface (Fig. 1). Clearly the space occupied by an atom is defined by the union of a given attractor and its associated basin or by its atomic surface.

Also shown in Figure 1 are the pairs of gradient paths which originate at a $(3,-1)$ critical point and terminate at neighboring attractors. Each such pair of trajectories is defined by the eigenvector associated with the unique positive eigenvalue of a $(3,-1)$ critical point. These two gradient paths define a line through the charge distribution along which $\rho(\mathbf{x})$ is a maximum with respect to any lateral displacement. Such a line is call a *bond path*.

For a given configuration $\mathbf{X}$ in nuclear configuration space, a *molecular graph* is defined as the union of the closures of the bond paths. Pictorially the molecular graph is the network of bond paths linking pairs of neighboring nuclear attractors.

The remaining critical points of rank three, $(3,+1)$ and $(3,+3)$ critical points, occur as consequences of particular geometrical arrangements of bond paths and define the remaining elements of molecular structure—rings and cages. The eigenvectors associated with the two positive eigenvalues of the Hessian matrix of a $(3,+1)$ critical point generate an infinite set of gradient paths which originate at the critical point and which define a surface called the ring surface. The remaining eigenvector generates a pair of gradient paths which terminate at the critical point and define a unique axis perpendicular to the ring surface at the critical point. A ring, as an element of structure, is defined as a part of a molecular graph which bounds a ring surface.

The eigenvectors associated with a $(3,+3)$ critical point, a local minimum in $\rho(\mathbf{x})$, generate an infinity of gradient paths which originate at the critical point and define a bounded region of space. A cage, as the final element of molecular structure, is a part of a molecular graph which contains at least two rings, such that the union of the ring surfaces bounds a region of R^3 which contains a $(3,+3)$ critical point.

III. ATOMIC PROPERTIES

By appealing to quantum mechanics one finds that the zero-flux surface conditions, eq. (4), which is a corollary of the topological definition of an atom, leads to a variational definition of its average properties.[3] For the present purpose we need point out but one consequence of this definition, namely, that any atomic property F is the average over the atomic basin of an effective single-particle density $f(\mathbf{x})$. Thus the value of the property F for atom Ω is

$$F(\Omega) = \int_{\Omega} f(\mathbf{x})\, d\mathbf{x} \qquad (5)$$

It follows from this definition that the average value of F for a total molecular system is given by the sum, over the atoms in the molecule, of the corresponding atomic values:

$$F = \sum_{\Omega} F(\Omega) \qquad (6)$$

The evaluation of $F(\Omega)$ is a nontrivial problem since the atomic surface which bounds the region Ω does not in general have a local definition, much less a simple geometrical structure. We have previously reported on a method of integration which avoids the direct determination of the atomic surface by the implementation of the definition of an atom as the union of an attractor and its basin.[5] By integrating along the trajectories of $\nabla \rho(\mathbf{x})$ which terminate at a given nucleus, one must necessarily cover the basin of an atom. In addition, because of the zero-flux surface condition [eq. (4)] it is impossible to cross an interatomic surface into the basin of a neighboring atom. To exploit this idea requires a coordinate transformation from (x,y,z) to (s,θ,ϕ) where the parameter s, eq. (1), determines the position of a point along the gradient path which is defined by some initial set of angular coordinates, θ and ϕ.

An integration program implementing this algorithm is efficient in the determination of the average properties of atoms with a single interatomic surface. However, in cases where a given atom is bonded to two or more different neighboring atoms, the times necessary to obtain the required numerical accuracy can become unacceptably large. This is particularly true in those cases in which the charge distribution is relatively flat in the neighborhood of a bond critical point where the path parameter s attains a limiting value of minus infinity.

The algorithm described here involves the direct determination of the atomic surface bounding a given atom. This is accomplished by determining the coordinates of a spaced set of points along gradient paths which terminate at a given $(3,-1)$ bond critical and which thus lie in an interatomic surface. The portion of the surface lying between
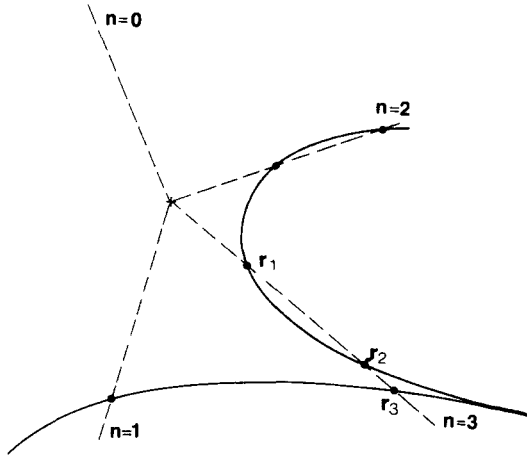
Figure 2. An illustration of four rays $R(\theta,\phi)$ (dashed lines) originating at the nucleus, each of which intersects the atomic surface n times for $n = 0, 1, 2$, and 3. The points of intersection for one ray, the set $\{r_1, r_2, \ldots, r_n\}$ are shown for the case $n = 3$.

two such neighboring trajectories is then represented approximately by a piecewise linear function.

IV. ALGORITHM

With the introduction of a spherical coordinate system centered at the nucleus, eq. (5) becomes

$$\int_{\Omega} f(\mathbf{x})\, d\mathbf{x} = \int_0^{2\pi} \int_0^{\pi} \int_{I_{\Omega}(\theta,\phi)}$$

$$\times f(r,\theta,\phi) r^2 \sin\theta \, dr \, d\theta \, d\phi \quad (7)$$

The symbol $I_{\Omega}(\theta,\phi)$ denotes the integration interval of r. The evaluation of $F(\Omega)$ is thus dependent upon the evaluation of $I_{\Omega}(\theta,\phi)$ as the limits of integration of the angular variables are known. We now describe an algorithm for the calculation of $I_{\Omega}(\theta,\phi)$.

A given pair of angles (θ,ϕ) define a ray $R(\theta,\phi) = \{(r,\theta,\phi), r \geq 0\}$, originating at the nuclear position. The integration interval of r is then

$$I_{\Omega}(\theta,\phi) = \{r,(r,\theta,\phi) \in \Omega \cap R(\theta,\phi)\} \quad (8)$$

To determine $I_{\Omega}(\theta,\phi)$ it is sufficient to determine the elements of the set

$$S_{\Omega}(\theta,\phi) = \{r,(r,\theta,\phi) \in S_{\Omega} \cap R(\theta,\phi)\}$$

In general, a given ray may intersect the atomic surface n times (see Fig. 2). Denoting a point of intersection by r_i, the set of intersections for a given ray is

$$S_{\Omega}(\theta,\phi) = \{r_1, r_2, \ldots, r_n\} \quad (9)$$

and, correspondingly, the interval $I_{\Omega}(\theta,\phi)$ is one of the following:

$$I_{\Omega}(\theta,\phi) = \begin{cases} \{r \text{ with } 0 \leqslant r < r_1 \text{ or } r_2 < r < r_3 \cdots \\ \quad \text{or } r_n < r < \infty\} \text{ if } n \neq 0 \text{ and even} \\ \{r \text{ with } 0 \leqslant r < r_1 \cdots \text{ or } r_{n-1} \\ \qquad\qquad\qquad < r < r_n\} \text{ if } n \text{ odd} \\ \{r, r \geqslant 0\} \text{ if } n = 0 \end{cases}$$

It is unusual for the set $S_{\Omega}(\theta,\phi)$ to contain more than three elements.

The problem of evaluating $F(\Omega)$ by eq. (7) has thus been reduced to the determination of $S_{\Omega}(\theta,\phi)$, the points of intersection of a given ray with the atomic surface.

Determination of $S_{\Omega}(\theta,\phi)$

As discussed in Sec. II, the interatomic surface S_{AB} between two neighboring nuclei A and B is generated by the two eigenvectors $\mathbf{v}_1$ and $\mathbf{v}_2$ associated with the negative roots of the Hessian matrix $H(\rho)$ of the $(3,-1)$ critical point at $\mathbf{x}_c$. Denoting by ϵ the length of a vector with origin at $\mathbf{x}_c$, one may write

$$S_{AB} = \lim_{\epsilon \to 0^+} S_{AB}^{\epsilon} \quad (10)$$

where $S_{AB}^{\epsilon} = \{\mathbf{x}, \mathbf{x}$ is a solution to eq. (3) with initial values $\mathbf{x}_\alpha = \mathbf{x}_c + \epsilon(\mathbf{v}_1 \cos\alpha + \mathbf{v}_2 \sin\alpha) \; \forall \; \alpha \in [0,2\pi]\}$. The length ϵ is typically taken to be 1×10^{-4} a.u. Such a value for ϵ is sufficient to generate gradient paths which terminate at the $(3,-1)$ critical point, i.e., they lie in S_{AB} within the required numerical accuracy. With this approximation to S_{AB} by S_{AB}^{ϵ}, we now discuss the approximation to S_{AB}^{ϵ} by a piecewise linear function.

Consider two gradient paths in S_{AB}^{ϵ} and a number of points on each of them where the points are chosen to be equidistant in terms of the path length l (Fig. 3). The area between the two paths can be divided into triangles: $\Delta(\mathbf{x}_i, \mathbf{x}_j, \mathbf{x}_k)$. Through the introduction of N gradient paths with initial values $x_{\alpha_0}, x_{\alpha_1}, \ldots, x_{\alpha_N} = x_{\alpha_0}$ and $\alpha_i = 2\pi i/N$, the whole surface can thus be partitioned into nonoverlapping triangles. The algorithm developed here is to determine whether or not a given ray $R(\theta,\phi)$ intersects a particular triangle $\Delta(\mathbf{x}_1, \mathbf{x}_2, \mathbf{x}_3)$.

In the following it is assumed that the triangle under consideration $\Delta(\mathbf{x}_1, \mathbf{x}_2, \mathbf{x}_3)$, is nondegenerate, i.e., its associated matrix $\mathbf{A} \, (\mathbf{x}_1|\mathbf{x}_2|\mathbf{x}_3)$ is nonsingular. The surface S_{AB}^{ϵ} is locally approximated by the plane containing $\mathbf{x}_1$, $\mathbf{x}_2$, and $\mathbf{x}_3$. The general equation for a plane is

$$P(\mathbf{x}) = ax + by + cz + d = 0 \quad (11)$$

Three of the four constants in eq. (11) are fixed by demanding that the coordinates of the three vertices be in the plane

$$P(\mathbf{x}_1) = P(\mathbf{x}_2) = P(\mathbf{x}_3) = 0$$

and d, which may be arbitrarily assigned any nonzero value since the plane does not contain the origin, is set equal to -1. To determine whether a given ray intersects this particular triangle we first consider the plane defined by the origin $\mathbf{0}$ (at the nucleus of the atom) and two of the vertices of the triangle, say $\mathbf{x}_2$ and $\mathbf{x}_3$. If $R(\theta,\phi)$ is to intersect the triangle, then it must be situated on the same side of this plane as $\mathbf{x}_1$. This yields a necessary condition for intersection. By demanding the same condition for the planes formed from $(\mathbf{0},\mathbf{x}_1,\mathbf{x}_3)$ and $(\mathbf{0},\mathbf{x}_1,\mathbf{x}_2)$ we have three necessary conditions for intersection, and since the ray is now bounded by all three sides of the triangle, the conditions are also sufficient.

Let $h_1(\mathbf{x})$ denote the equation of the plane containing the origin $\mathbf{0}$ and $\mathbf{x}_2$ and $\mathbf{x}_3$,

$$h_1(\mathbf{x}) = a_1x + b_1y + c_1z = 0 \qquad (12)$$

Since the vector constructed from the coefficients in eq. (12) is normal to the plane they define, one obtains the following three relations:

$$(a_1,b_1,c_1) \cdot \mathbf{x}_2 = (a_1,b_1,c_1) \cdot \mathbf{x}_3 = 0$$

and

$$(a_1,b_1,c_1) \cdot \mathbf{x}_1 = 1$$

The nonzero value assigned to the final dot product above is arbitrary [if $h_1((\mathbf{x}_1) \neq 0$]; it is set equal to unity for convenience. The matrix formulation of these three equations is

$$(a_1,b_1,c_1) \cdot \mathbf{A} = (1,0,0) \qquad (13)$$

A necessary condition for a given ray $R(\theta,\phi)$ to be situated on the same side of the plane $h_1(\mathbf{x})$ as $\mathbf{x}_1$ requires that

$$h_1(\mathbf{x}_1)h_1(\hat{\mathbf{x}}) = h_1(\hat{\mathbf{x}}) \geq 0 \qquad (14)$$

where $\hat{\mathbf{x}}$ is a vector of unit length along the ray $R(\theta,\phi)$,

$$\hat{\mathbf{x}} = \begin{pmatrix} \sin\theta\cos\phi \\ \sin\theta\sin\phi \\ \cos\phi \end{pmatrix} \in R(\theta,\phi)$$

This condition is also sufficient, because if $h_1(\hat{\mathbf{x}}) < 0$, there is a point $\mathbf{x}$ on the line between $\hat{\mathbf{x}}$ and $\mathbf{x}_1$ with $h_1(\mathbf{x}) = 0$, implying that $\mathbf{x}_1$ and $\hat{\mathbf{x}}$ are situated on different sides of the plane.

Similar equations are obtained using the planes defined by the points $\mathbf{0},\mathbf{x}_1,\mathbf{x}_3$ and $\mathbf{0},\mathbf{x}_1,\mathbf{x}_2$:

$$h_2(\mathbf{x}) = a_2x + b_2y + c_2z = 0$$

$$h_3(\mathbf{x}) = a_3x + b_3y + c_3z = 0$$

Corresponding to eq. (13), these two planes define normal vectors with the properties

$$(a_2,b_2,c_2) \cdot \mathbf{A} = (0,1,0) \qquad (15)$$

$$(a_3,b_3,c_3) \cdot \mathbf{A} = (0,0,1) \qquad (16)$$

and one obtains two more necessary conditions which must be satisfied if a given ray $R(\theta,\phi)$ is to intersect the triangle $\triangle(\mathbf{x}_1,\mathbf{x}_2,\mathbf{x}_3)$:

$$h_2(\hat{\mathbf{x}}) \geq 0 \qquad (17)$$

$$h_3(\hat{\mathbf{x}}) \geq 0 \qquad (18)$$

Equations (14), (17), and (18) taken together constitute a necessary *and* sufficient condition for $R(\theta,\phi)$ to intersect the triangle in question.

Equations (13), (15), and (16) as well as (14), (17), and (18) can be written in the more convenient matrix form:

$$\begin{pmatrix} a_1 & b_1 & c_c \\ a_2 & b_2 & c_2 \\ a_3 & b_3 & c_3 \end{pmatrix} \cdot \mathbf{A} = \begin{pmatrix} 1 & 0 & 0 \\ 0 & 1 & 0 \\ 0 & 0 & 1 \end{pmatrix} = \mathbf{A}^{-1} \cdot \mathbf{A}$$

and

$$\begin{pmatrix} a_1 & b_1 & c_1 \\ a_2 & b_2 & c_2 \\ a_3 & b_3 & c_3 \end{pmatrix} \cdot \hat{\mathbf{x}} = \mathbf{A}^{-1} \cdot \hat{\mathbf{x}}$$

$$= \begin{pmatrix} h_1(\hat{\mathbf{x}}) \\ h_2(\hat{\mathbf{x}}) \\ h_3(\hat{\mathbf{x}}) \end{pmatrix} = h \geq 0 \qquad (19)$$

Because of the nondegeneracy of $\triangle(\mathbf{x}_1,\mathbf{x}_2,\mathbf{x}_3)$, at least one of the components of h is nonzero.

When eq. (19) is satisfied for a given ray and a particular triangle, then the point of intersection of the ray with the plane of the triangle $P(\mathbf{x})$ must be determined. Since d in eq. (11) for $P(\mathbf{x})$ is set equal to -1, one has

$$(a,b,c) \cdot \mathbf{A} = (1,1,1)$$

or

$$(a,b,c) = (1,1,1) \cdot \mathbf{A}^{-1} \qquad (20)$$

Since $|\hat{\mathbf{x}}| = 1$, a point on $R(\theta,\phi)$ has the form $r\hat{\mathbf{x}}$ where r is the distance from the point to the origin.

If we denote by $r(\theta,\phi)$ the distance to the plane of the triangle $\triangle(\mathbf{x}_1,\mathbf{x}_2,\mathbf{x}_3)$, then

$$P[r(\theta,\phi)\hat{\mathbf{x}}] = (a,b,c)r(\theta,\phi) \cdot \hat{\mathbf{x}} - 1 = 0$$

which, using eqs. (19) and (20), may be rewritten as

$$r(\theta,\phi)(1,1,1) \cdot h - 1 = 0$$

Thus the desired element of $S_\Omega(\theta,\phi)$ is given by

$$r(\theta,\phi) = [h_1(\hat{\mathbf{x}}) + h_2(\hat{\mathbf{x}}) + h_3(\hat{\mathbf{x}})]^{-1} \quad (21)$$

Because of eq. (19) and the nondegeneracy of $\triangle(\mathbf{x}_1,\mathbf{x}_2,\mathbf{x}_3)$, $r(\theta,\phi)$ is both positive and finite.

The algorithm for the determination of the set $S_\Omega(\theta,\phi)$ may be summarized as follows.

1. Compute $\hat{\mathbf{x}} \in R(\theta,\phi)$ with $|\hat{\mathbf{x}}| = 1$.
2. Calculate equidistant points on the gradient path p_0 defined by the initial value problem

$$\frac{dx}{dl} = \frac{\nabla\rho}{|\nabla\rho|}, \quad \mathbf{x}_0 = \mathbf{x}_\epsilon + \epsilon \cdot \mathbf{v} \quad (\alpha_0 = 0)$$

3. Repeat step 2 for N paths labelled $i = 1,\ldots,N$. If $i < N$ calculate equidistant paths on p_i with initial values.

$$\mathbf{x}_i = \mathbf{x}_c + \epsilon(\mathbf{v}_1 \cdot \cos\alpha_i + \mathbf{v}_2 \sin\alpha_i)$$
$$\text{and } \alpha_i + 2\pi i/N.$$

For $i = N$, set $p_N = p_0$.

4. Partition the area between p_{i-1} and p_i into triangles (Fig. 3).
5. For each triangle $\triangle(\mathbf{x}_i,\mathbf{x}_j,\mathbf{x}_k)$ solve the linear system

$$(\mathbf{x}_i \,|\, \mathbf{x}_j \,|\, \mathbf{x}_k) \cdot h = \mathbf{A} \cdot h = \hat{\mathbf{x}}$$

which follows from eq. (19).

6. If $h \geq 0$ compute an element of $S_\Omega(\theta,\phi)$ with eq. (21).

Typically one chooses 48 ϕ planes and 32 θ values for each ϕ plane. The intersection of each of the 48 $\times$ 32 rays thus generated are determined by steps 5 and 6.

To guarantee a continuous distribution of gradient paths and thus a continuous accuracy in the approximation of the surface through S'_{AB}, another gradient path should be inserted if the Euclidean distance d between the last points of p_{i-1} and p_i exceeds a certain length. The initial angle of the inserted path can, for example, be chosen as $\bar{\alpha} = \frac{1}{2}(\alpha_i + \alpha_{i-1})$. This test should be repeated using p_{i-1} and $p_{\bar{\alpha}}$ until d is sufficiently small.

In the case of a linear molecule the algorithm can be simplified considerably. Since the molecule
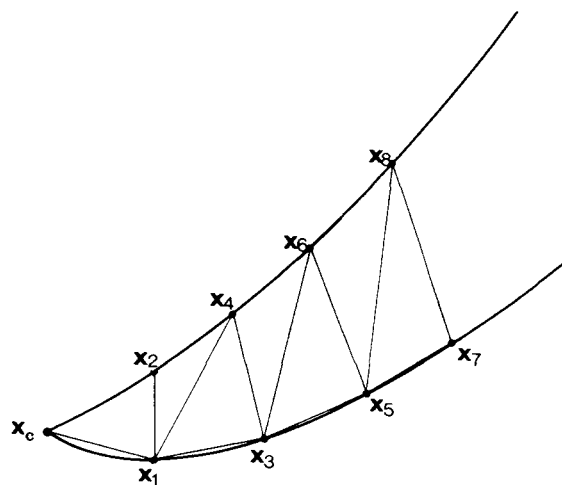

Figure 3. Two trajectories of $\nabla\rho$ which terminate at a $(3,-1)$ critical point and belong to the set S'_{AB}. The approximation to the portion of the interatomic surface S_{AB} lying between these two trajectories through a set of triangles formed by linking equidistant points (in terms of the path length ℓ) on each trajector is illustrated.

has cylindrical symmetry it is only necessary to compute a single path in the surface. Instead of partitioning the whole surface into triangles it is sufficient to approximate this path using piecewise linear functions (line segments). All planes in the previous development of the algorithm reduce to lines and the 3 $\times$ 3 system in step 5 reduces to a 2 $\times$ 2 system.

V. RINGS AND CAGES

The algorithm described in Sec. III applies directly if the interatomic surface contains only $(3,-1)$ critical points. However, if the bond paths linking Ω to the rest of the molecule are part of a ring or cage structure, then two or more of its interatomic surfaces will contain $(3,+1)$ or $(3,+1)$ and $(3,+3)$ critical points in addition to the $(3,-1)$ critical point. If the interatomic surface S_{AB} occurs in a ring structure, then one of the gradient paths which terminates at the $(3,-1)$ critical point and lies in S_{AB} originates at the $(3,+1)$ or ring critical point and is of finite length [see Figs. 1(A) and 1(B)]. In the case of a cage structure, S_{AB} will contain two such trajectories in addition to a set of trajectories which originate at the $(3,+3)$ or cage critical point [Fig. 1(C)]. It is clear from Figure 4 that the pair of gradient paths at the critical angles α_i and α_{i-1}, which bracket the trajectory p_γ originating at a ring critical point at $\mathbf{x}'_c$, diverge in the neighborhood of $\mathbf{x}'_c$. Thus even for small initial values of $|\alpha_i - \alpha_{i-1}|$ the end points of the associated trajectories p_i and p_{i-1} diverge. Because of
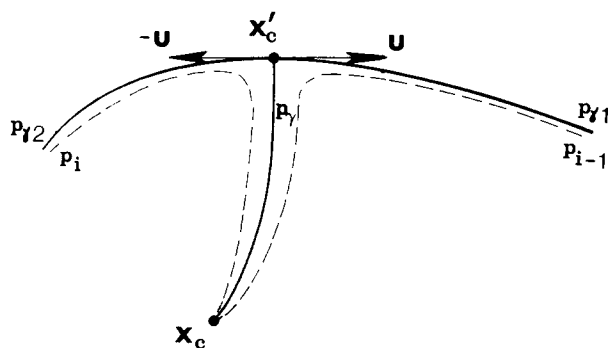
Figure 4. The trajectory p_γ which originates at a $(3,+1)$ critical point at $\mathbf{x}_c'$ and terminates at the $(3,-1)$ critical point at $\mathbf{x}_c$. The trajectories p_i and p_{i-1} are for the critical starting angles α_i and α_{i-1} which bracket the value of $\alpha = \gamma$ which would generate p_γ. The vector $\mathbf{u}$ is associated with the negative root of the Hessian of ρ at $\mathbf{x}_c'$. It is tangent to $p_{\gamma 1}$ and $p_{\gamma 2}$ at $\mathbf{x}_c'$.

Figure 5. A diagram illustrating the iteration process used in the determination of the initial angle γ which defines the trajectory p_γ.

this behavior it is no longer possible to partition the surface element between them into triangles as the triangles may overlap or become degenerate. To overcome this problem, one must specifically include the ring trajectory p_γ in the set S_{AB}^ϵ.

The initial values of p_γ, as for other trajectories in the surface, depend upon a linear combination of $\mathbf{v}_1$ and $\mathbf{v}_2$:
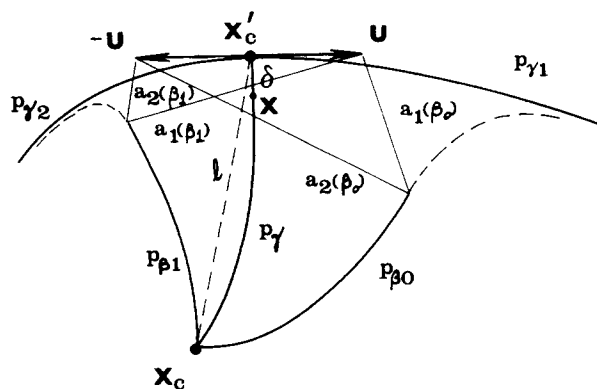
$$\mathbf{x}_\gamma = \mathbf{x}_c + \epsilon(\mathbf{v}_1 \cos \gamma + \mathbf{v}_2 \sin \gamma)$$

It is thus necessary to develop an algorithm for the determination of the initial angle γ. This is done by using the properties of the ring critical point at $\mathbf{x}_c'$. The vector μ_1 associated with the single negative root of $H(p)$ at $\mathbf{x}_c'$ generates two trajectories, $p_{\gamma 1}$ and $p_{\gamma 2}$, which lie on the unique axis of the $(3,+1)$ critical point (Fig. 4). Also, in the immediate neighborhood of $\mathbf{x}_c'$, the angle between p_γ and μ_1 equals $90°$. Thus for a point $\mathbf{x}$ on p_γ with $|\mathbf{x}_c' - \mathbf{x}| = \delta$, the function

$$g(\gamma) = |\mathbf{x}_c' + \mu_1 - \mathbf{x}| - |\mathbf{x}_c' - \mu_1 - \mathbf{x}|$$
$$= a_1(\gamma) - a_2(\gamma) = 0(\delta^2)$$

approaches zero as does δ^2. Using these properties of the ring critical point, it is possible to set up an iteration process for γ by searching for zeroes in $g(\gamma)$.

1. Compute the geometrical length l between $\mathbf{x}_c$ and $\mathbf{x}_c'$ (see Fig. 5).
2. (a) Pick two initial angles β_0, β_1 with $\beta_0 < \gamma < \beta_1$.
   (b) Compute the paths p_{β_0} and p_{β_1} with initial angles β_0 and β_1, starting at $\mathbf{x}_c$ and with path lengths equal to l where $l \le$ path length of p_γ.

(c) Calculate $g(\beta_0)$ and $g(\beta_1)$ for the end points of p_{β_0} and p_{β_1}. Then $g(\beta_0) \le 0 \le g(\beta_1)$.

3. (a) Compute
   $$\beta = [\beta_0 g(\beta_1) - \beta_1 g(\beta_0)/(g(\beta_1) - g(\beta_0)]$$
   This is the formula of a *regula falsi* iteration process to find the zeroes of g.
   (b) Compute the path p_β up to the length l and $g(\beta)$ for the end point of p_β.
   (c) If:
   $g(\beta)$ is sufficiently small, set $\gamma = \beta$;
   $g(\beta) > 0$, set $\beta_1 = \beta$ and go to iteration 3(a);
   $g(\beta) < 0$, set $\beta_0 = \beta$ and go to iteration 3(a):

The path length from $\mathbf{x}_c$ to $\mathbf{x}$ is l and hence the final δ is the path length from $\mathbf{x}$ to $\mathbf{x}_c'$. This algorithm usually converges in three to six steps, depending on the curvature of p_γ.

Once p_γ is determined, the area between p_{i-1} and the combined paths p_γ and $p_{\gamma 1}$ is partitioned into triangles, as is the area lying between p_i and the combined paths p_γ and $p_{\gamma 2}$. Integrations over the basins of atoms in ring and cage structures are included in the examples discussed below.

Surface Integrations

The whole scheme of fitting an interatomic surface S_{AB} by a partitioning into triangles Δ_i, $i = 1, \ldots, K$, may also be used to integrate a density $f(\mathbf{x})$ over an interatomic surface S_{AB}:

$$\int_{S_{AB}} f(x)dx = \lim_{\epsilon \to 0^+} \int_{S_{AB}^\epsilon} f(x)dx$$

and

$$\int_{S_{AB}^\epsilon} f(x)dx = \lim_{K \to \infty} \sum_{i=1}^{K} A(\Delta_i)f(\Delta_i) \quad (22)$$

Table I. Atomic properties of hydrocarbons.[a]

Molecule	Atom Ω	N(Ω)	K(Ω)	L(Ω)×10³
Ethane	H	1.0758	0.6885	0.09
C_2H_6	C	5.7714	36.7710	1.29
	Integrated totals	17.9975	77.6732	3.12
	SCF totals	18.0000	77.6725	0
	error	2.5×10^{-3}	7×10^{-4}	3.12
Propene	H1	1.0601	0.6710	-0.01
C_3H_6	H2	1.0576	0.6691	-0.03
	H3	1.0652	0.6772	0.04
	H4	1.0636	0.6803	0.11
	H5(6)	1.0605	0.6778	0.09
	C1	5.6082	36.8180	2.01
	C2	6.2331	37.1913	-4.99
	C3	5.7956	36.7787	-3.19
	Integrated totals	24.0044	114.8412	-5.88
	SCF totals	24.0000	114.8427	0
	error	4.4×10^{-3}	1.5×10^{-3}	-5.88
Cyclopropene	H1(2)	0.9760	0.6067	-0.05
C_3H_4	H3(4)	1.0776	0.6917	0.06
	C1(2)	6.0782	37.1703	0.60
	C3	5.7350	36.7626	0.02
	Integrated totals	21.9986	113.7000	1.26
	SCF totals	22.0000	113.7000	0
	error	1.4×10^{-3}	$<1 \times 10^{-4}$	1.26
Cyclopropenium cation	H	0.7268	0.4438	0.10
$C_3H_3^+$	C	5.9397	36.8623	0.00
	Integrated totals	19.9997	111.9184	0.30
	SCF totals	20.0000	111.9183	0
	error	3×10^{-4}	1×10^{-4}	0.30
Tetrahedrane	H	0.9615	0.5980	0.01
C_4H_4	C	6.0388	37.0892	-0.10
	Integrated totals	28.0012	150.7488	-0.36
	SCF totals	28.0000	150.7479	0
	error	1.2×10^{-3}	9×10^{-4}	-0.36

[a] All properties are in a.u. The atoms are identified in Fig. 6.

where $A(\Delta_i)$ denotes the area of triangle Δ_i and $f(\Delta_i)$ the value of the density f at any point inside Δ_i. The limit on the r.h.s. of eq. (22) has to be taken such that

$$\lim_{K \to \infty} A(\Delta_i) = 0; \ \forall i$$

and each triangle approaches a point in the surface.

The ability to calculate the average value of a property over an atomic surface is essential to the theory of atoms in molecules because of the atomic statement of the hypervirial theorem. This theorem relates the atomic average of the commutator of the Hamiltonian and an operator **A** to an integral over the atomic surface:

$$\{<[\hat{H},\hat{A}] >_\Omega + \text{c.c.}\}$$
$$= \{(-\hbar^2/2m) \oint dS(\mathbf{x}_1) \int d\mathbf{x}'[\nabla_1\psi^*(\hat{A}(\mathbf{x}_1)\psi$$
$$- \psi^*\nabla_1(\hat{A}(\mathbf{x}_1)\psi)] \cdot \mathbf{n}(\mathbf{x}_1) + \text{c.c.}\} \quad (23)$$

The symbol $\int dx'$ denotes the integration over the coordinates of all the electrons but those of electron 1. Thus an atomic property is either determined directly by a surface quantity or it is related

to another atomic property by a surface quantity.

VI. NUMERICAL EXAMPLES

This theory of molecular structure has recently been applied to a study of the hydrocarbons.[6,7] Integration results for some of the molecules whose properties are discussed in that study are used to illustrate the implementation of the algorithms developed here. We report in Table I atomic integrations of three properties for each set of equivalent atoms in five molecules, which include examples of open chain, ring, and cage structures. This enables one to compare, using eq. (6), the integrated value for each molecular property expressed as a sum of atomic contributions with the corresponding values obtained in the original SCF calculation. The atoms are identified in the molecular graphs shown in Figure 6. To illustrate the range of atomic properties which may be calculated by this method we report in Table II the average values of a number of atomic properties for a hydrogen atom in the ethane molecule. Also given are the values for some of the same properties integrated over the interatomic surfaces of this molecule. Since the values of properties integrated over the basin and surface of an atom are related by the atomic hypervirial theorem, one obtains further checks on the accuracy of the method of integration presented here.

The atomic properties reported in Table I are (i) the average electron population:

$$N(\Omega) = \int_\Omega d\mathbf{x} \, \rho(\mathbf{x}) \quad (24)$$

and (ii) the average atomic kinetic energy. This quantity may be obtained by integration of either of two expressions, $K(\mathbf{x})$ or $G(\mathbf{x})$, for the kinetic energy density. They are defined as

$$K(\mathbf{x}) = -\tfrac{1}{2}\nabla \cdot \nabla\Gamma(\mathbf{x},\mathbf{x}')|_{\mathbf{x}=\mathbf{x}'} \quad (25)$$

and

$$G(\mathbf{x}) = \tfrac{1}{2}\nabla \cdot \nabla'\Gamma(\mathbf{x},\mathbf{x}')|_{\mathbf{x}=\mathbf{x}'} \quad (26)$$
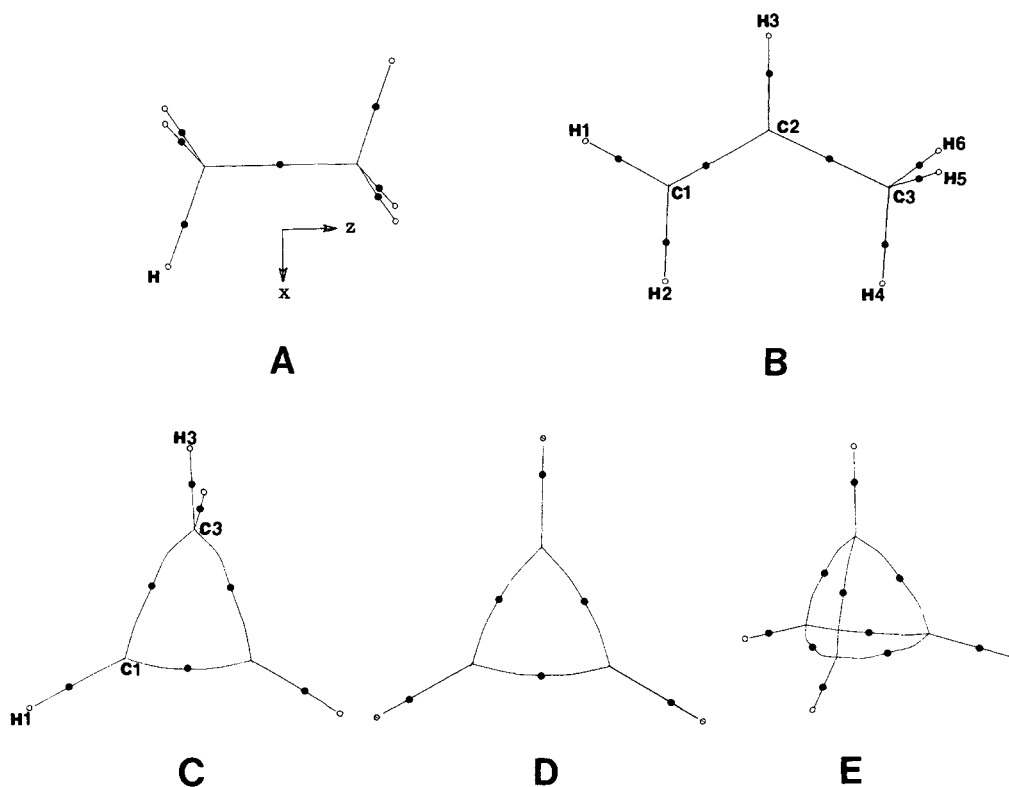
where

$$\Gamma(\mathbf{x},\mathbf{x}') = n\int ds_1 \ldots ds_n \int d\mathbf{x}_2 \, d\mathbf{x}_3 \ldots$$
$$\times d\mathbf{x}_n \Psi^*(\mathbf{x},\mathbf{x}_2 \ldots \mathbf{x}_n)\Psi(\mathbf{x}',\mathbf{x}_2 \ldots \mathbf{x}_n) \quad (27)$$

is the first-order density matrix. The kinetic energy densities $K(\mathbf{x})$ and $G(\mathbf{x})$ differ from one another by the term $L(\mathbf{x})$ where

$$L(\mathbf{x}) = K(\mathbf{x}) - G(\mathbf{x}) = -\tfrac{1}{4}\nabla^2\rho(\mathbf{x}) \quad (28)$$

Figure 6. Planar projections of the molecular graphs for the molecules listed in Table I: A, C_2H_6; B, C_3H_6; C, C_3H_4; D, $C_3H_3^+$; E, C_4H_4. The hydrogen atom in A whose properties are given in Table II is the one denoted by H in the xz plane.

The integral of the density $L(\mathbf{x})$ over an atomic basin equals zero, as a direct consequence of the zero-flux boundary condition, eq. (4). Thus the vanishing of $L(\Omega)$, the atomic integral of $L(\mathbf{x})$, is a measure of how well the atomic surface is approximated and it provides a test of the accuracy of the integration method over each individual atom.

The integration program PROAIM which implements the algorithms described above is designed to handle wavefunctions obtained using either STO or GTO basis functions. The molecules studied here are single determinantal functions constructed from an STO-3G basis, at their equilibrium geometries.

The program PROAIM requires as input information the number, type, and coordinates of critical points contained in the atomic surface of atom Ω. This information is calculated by the program EXTREME. In the evaluation of $F(\Omega)$ by eq. (7), the integration is split into two contributions. The first integration is over the volume of the largest sphere M contained within γ, i.e., the radius β of M is set equal to the distance from the nucleus of Ω to the nearest $(3,-1)$ critical point in the atomic surface of Ω. If $\beta < 1.5$ a.u., the integration uses a 48-point Gaussian quadrature in r.

If $\beta > 1.5$ a.u., a 64-point Gaussian quadrature is used. The integration along a given ray between $\beta < r < r(\theta,\phi)$ again uses a Gaussian quadrature with the number of points, lying between 8 and 54, being determined by this remaining length D of the ray. Integration along a given ray is followed first by an integration over θ and then by one over ϕ. The integrations over the angles also make use of a Gaussian quadrature.

The errors in $L(\Omega)$, reported in Table I (it should integrate to zero for each atom separately), are least for the hydrogen atoms, atoms which have but one interatomic surface. With the exception of two of the carbon atoms in propene, the error in $L(\Omega)$ is such that the difference in the values of the average kinetic energy of an atom as determined by $K(\Omega)$ and $G(\Omega)$ is of the order of or less than 1 kcal/mol. One notes that the error in the sum of the atomic populations is of the same order as the magnitude of the sum of the errors in $L(\Omega)$.

The atomic properties listed in Table II following $N(\Omega)$, $G(\Omega)$, $K(\Omega)$, and $L(\Omega)$ are the following: VNEO is the potential energy of interaction of the nucleus of Ω with the atomic charge density; VNET is the total potential energy of interaction of all the nuclei in the molecule with the charge density of Ω; VEET is the electron–

Table II. Integrated properties of the H atom in C_2H_6.

Results of the Integration over Atom H1 in C_2H_6		The Atomic Overlap Matrix AOM H1									Results of the Integration Over the Interatomic Surface of H1 (atom A) and C1 (atom B)	
N	1.07580E+00	.000									N	9.84523E-01
G	6.88450E-01	.000	.000								G	5.96559E-01
K	6.88543E-01	.000	-.000	.048							K	4.02008E-01
L	9.29025E-05	.000	.000	-.060	.078						L	-1.94551E-01
VNEO	-1.38586E+00	.000	.000	-.000	.000	.006					GRN	3.63498E-05
VNET	-7.12351E+00	-.000	-.000	.088	-.109	-.000	.164				RA(-1)	7.81233E-01
VEET	2.89786E+00	-.000	-.000	.037	-.051	-.000	.068	.038			RA0	9.52041E-01
DX	-8.19521E-02	-.000	-.000	.000	-.000	.005	.000	.000	.005		RA1	1.27058E+00
DY	-2.29263E-06	.000	.000	-.096	.122	.000	-.180	-.077	-.000	.200	RA2	1.90872E+00
DZ	3.57444E-02										RB(-1)	5.97240E-01
QXX	3.26137E-01			Nα	5.37900E-01						RB0	9.59871E-01
QXY	-7.51355E-06			Nβ	5.37900E-01						RB1	1.62957E+00
QXZ	-1.93089E-01			N	1.07580E+00						RB2	2.94422E+00
QYY	-2.12277E-01			FOOα	-2.64632E-01						R(-1)	1.37847E+00
QYZ	-7.19132E-06			FOOβ	-2.64632E-01						R0	1.91191E+00
QZZ	-1.13860E-01			FOO	-5.29264E-01						R1	2.90015E+00
FAXA	-1.91722E-01			LOCα	4.91973E-01						R2	4.85294E+00
FAYA	4.17484E-07			LOCβ	4.91973E-01						VA	-1.53396E-01
FAZA	7.31011E-02			FLα	2.73268E-01						VB	-5.43146E-04
FBXA	1.61000E+00			FLβ	2.73268E-01						V	-1.53939E-01
FBYA	1.00571E-06			FL	5.46535E-01						SGNX	7.00522E-02
FBZA	-8.96737E-01										SGNY	1.29198E-06
R(-1)	1.38586E+00										SGNZ	-2.68194E-02
R1	1.15027E+00											
R2	1.57786E+00											
GR(-1)	-1.99024E+00											
GR0	-2.27502E+00											
GR1	-3.32986E+00											
GR2	-5.97871E+00											
I	3.40115E-01											

electron repulsion energy for atom Ω; DX, DY, and DZ are the atomic dipole moments of Ω with nucleus as origin; the Q values are the components of the (traceless) quadrupole moment tensor for atom Ω, again with nucleus as origin; FAXA, FAYA, and FAZA are the components of the Hellmann–Feynman force exerted on the nucleus of Ω by the charge density of Ω; the corresponding quantities FBXA are the net components of the forces exerted on all remaining nuclei in the molecule by the charge density in Ω; R(−1), R1, and R2 are the averages over the atomic charge density of the operators r^{-1}, r, and r^2, where r is the radial distance from the nucleus; GR(−1), GR0, GR1, and GR2 are the averages of the quantities $(1/r)\mathbf{x} \cdot \nabla\rho$, $\mathbf{x} \cdot \nabla\rho$, $r\mathbf{x} \cdot \nabla\rho$, and $r^2\mathbf{x} \cdot \nabla\rho$ over the atomic basin and $I(\Omega)$ is the integral of $\rho' \ln \rho'$ where ρ' is the density normalized to unity.

The elements in the atomic overlap matrix are $S_{ij}(\Omega)$,

$$S_{ij}(\Omega) = \int_\Omega \phi_i \phi_j \, dx$$

where the ϕ_i are the molecular orbitals. For an RHF wavefunction, the $S_{ij}(\Omega)$ are the same for both the α and β spin orbitals. In general, these atomic overlaps determine (a) the atomic averages of the α and β electron populations,

$$N\alpha(\Omega) = \sum_i S_{ii}^\alpha(\Omega)$$

and (b) the atomic average of the Fermi correlation,

$$FOO\alpha(\Omega) = - \sum_{i,j} [S_{ij}^\alpha(\Omega)]^2$$

This latter quantity in turn determines the extent of localization of the α electrons in atom Ω (ref. 8),

$$LOC\alpha = |FOO\alpha(\Omega)|/N\alpha(\Omega)$$

and the fluctuation in the average α electron population,[8]

$$FL\alpha(\Omega) = \overline{[N\alpha(\Omega)]^2} - [\overline{N}\alpha(\Omega)]^2$$
$$= \overline{N}\alpha(\Omega) + FOO\alpha(\Omega)$$

The limiting value of $FOO\alpha(\Omega)$ is $-N\alpha(\Omega)$, as obtained for an isolated system. In this limiting case the fluctuation in $\overline{N}(\Omega)$ vanishes and the electrons are completely localized in Ω.[7] Both the localization of and the fluctuation in an electron population of an atom are *independent* of the molecular orbital representation (i.e., canonical set, some "localized" set, etc.) used to calculate the $S_{ij}(\Omega)$. They, as are all atomic properties, are determined solely by the state function of the system.

The surface properties, also listed in Table II, are for the interatomic surface associated with a CH bond in ethane. The new labels appearing in this list denote the following properties: GRN is the integral of $\nabla\rho(\mathbf{x})\cdot\mathbf{n}(\mathbf{x})$ over the interatomic

Table III. Test of numerical accuracy in satisfaction of eq. (29).

n in eq. (29)	Value of LHS of eq. (29) (volume integrations)	Value of RHS of eq. (29) (surface integration)	% difference
-1	0.7815	0.7812	3.8×10^{-2}
0	0.9524	0.9520	4.2×10^{-2}
1	1.2712	1.2706	4.7×10^{-2}
2	1.9106	1.9087	9.9×10^{-2}

surface. By eq. (4), this integral should vanish for an interatomic surface. The value reported here, $\sim 10^{-5}$, is typical and illustrates that the interatomic surface S_{AB} is numerically well approximated by the set S_{AB}^{ϵ}. RAn where $n = -1,0,1,2$ are the values of the integral

$$\oint dS(\mathbf{x}) r_A^n \rho(\mathbf{x}) \mathbf{x}_A \cdot \mathbf{n}_A(\mathbf{x})$$

The same quantities without the A or B labels are the sums of the corresponding values for A and B. VA, VB, and V are the virials of the forces exerted on the surface of atom A, atom B, and their sum, respectively, where, for example,

$$VA = \oint dS(\mathbf{x}) \mathbf{x}_A \cdot \vec{\sigma}(\mathbf{x}) \cdot \mathbf{n}_A(\mathbf{x})$$

The tensor $\vec{\sigma}(\mathbf{x})$ is the single-particle quantum mechanical stress tensor[2,3] which is totally determined by the first-order density matrix. The virial of the surface forces is related to the kinetic energy of atom $A [T(A) = K(A) = G(A)]$ and to the virial of the forces acting over the basin of the atom by the atomic virial theorem [$\hat{A} = -\mathbf{x} \cdot \nabla$ in eq. (23)],

$$2T(A) - \int_A \mathbf{x}_A \cdot \nabla \cdot \vec{\sigma}(\mathbf{x}) \, d\mathbf{x} = -VA$$

The total force exerted on the electrons of atom A is equal to the integral over its atomic surface of $\vec{\sigma}(\mathbf{x}) \cdot \mathbf{n}_A(\mathbf{x})$.[2,3] The final three entries in the table are the x, y, and z components of this force $\mathbf{F}(A)$ [$\hat{A} = -\nabla$ in eq. (23)],

$$\mathbf{F}(A) = \int_A d\mathbf{x}_1 \int d\mathbf{x}' \, \psi^*(-\nabla_1 \hat{V})\psi$$

$$= -\oint dS(\mathbf{x}) \vec{\sigma}(\mathbf{x}) \cdot \mathbf{n}_A(\mathbf{x})$$

where $\hat{V}$ is the total potential energy operator for the system. In words, $\mathbf{F}(A)$ is equal to the pressure exerted over the surface of the atom.

The atomic statement of the hypervirial theorem may be used to provide further tests of the accuracy of both the volume and surface integration results obtained by the program PROAIM. For operator $\hat{A} = r^{n+2}$ in eq. (23), the hypervirial theorem yields

$$(n + 3) \int_A r_A^n \rho(\mathbf{x}) d\mathbf{x} + \int_A r_A^n \mathbf{x}_A \cdot \nabla \rho(\mathbf{x}) d\mathbf{x}$$

$$= \oint dS \, r_A^n \rho(\mathbf{x}) \mathbf{x}_A \cdot \mathbf{n}_A(\mathbf{x}) \quad (29)$$

This expression holds for exact or approximate wavefunctions. Listed in Table III are the calculated values (using data given in Table II) for the l.h.s. and r.h.s. of eq. (23) for a number of n values. The percentage difference {100(l.h.s. − r.h.s.)/l.h.s.} is acceptably small for all values of n.

The importance of the atomic hypervirial theorem, eq. (23), lies in the fact that it relates an atomic property to an integral over the atomic surface S_A. If the atom A has n bonded neighbors, then S_A consists of n interatomic surfaces S_{AB} and correspondingly, the surface integral in eqs. (23) or (29) consists of a sum of n integrals, one over each S_{AB} in S_A. Thus summing eq. (29), for example, relates a sum of atomic properties to a sum of bond properties as there is one interatomic surface for each bonded pair of atoms in the molecule. Such a summation for the case $n = 0$ in eq. (29) yields

$$\sum_A \left\{ 3N(A) + \int_A r_A^n \mathbf{x}_A \cdot \nabla \rho(\mathbf{x}) d\mathbf{x} \right\}$$

$$= \sum_{A<B} \mathbf{R}_{AB} \cdot \oint_{AB} dS(\mathbf{x}) \rho(\mathbf{x}) \mathbf{n}_A(\mathbf{x}) \quad (30)$$

where the sum $A < B$ runs over each bonded pair of atoms in the molecule and $\mathbf{R}_{AB} = \mathbf{x}_A - \mathbf{x}_B$ is the vector from the nucleus of atom A to that of atom B. A surface integral of the kind appearing on the r.h.s. of eq. (30), divided by R_{AB}^2, has been shown to be proportional to the energy of the associated CH or CC bond in a hydrocarbon molecule.[7] Thus one may relate a bond property to a sum of atomic (i.e., volume) properties through an integral over the associated interatomic surface.

The programs EXTREME and PROAIM are to be submitted to the Quantum Chemistry Program Exchange. They are also available upon request.

References

1. R. F. W. Bader, S. G. Anderson, and A. J. Duke, *J. Am. Chem. Soc.*, **101**, 1389 (1979); R. F. W. Bader, T. T. Nguyen-Dang, and Y. Tal, *J. Chem. Phys.*, **70**, 4316 (1979).

2. R. F. W. Bader, *J. Chem. Phys.*, **73**, 2871 (1980); Y. Tal, R. F. W. Bader, T. T. Nguyen-Dang, M. Ojha, and S. G. Anderson, *J. Chem. Phys.*, **74**, 5162 (1981).

3. R. F. W. Bader and T. T. Nguyen-Dang, *Adv. Quantum*

Chem., **14,** 63 (1981).

4. R. F. W. Bader, T. T. Nguyen-Dang, and Y. Tal, *Rep. Prog. Phys.*, **44,** 893 (1981).

5. F. W. Biegler-König, T. T. Nguyen-Dang, Y. Tal, R. F. W. Bader, and A. J. Duke, *J. Phys. B*, **14,** 2739 (1981).

6. R. F. W. Bader, Ting-Hua Tang, Y. Tal, and F. W. Biegler-König, *J. Am. Chem. Soc.*, **104** (1982).

7. R. F. W. Bader, Ting-Hua Tang, Y. Tal, and F. W. Biegler-König, *J. Am. Chem. Soc.*, **104** (1982).

8. R. F. W. Bader and M. E. Stephens, *J. Am. Chem. Soc.*, **97,** 7391 (1975).